STRUCTURAL AND ELECTRON PARAMAGNETIC RESONANCE STUDIES OF $(ZrO)_{0.8}(Y_2O_3)_{0.2}$

N.L. SHUKLA[a], S.V. SHARMA[b], P. CHAND[b] AND B.N. MISRA[a]

[a] Department of Physics, Allahabad University, Allahabad, India
[b] Department of Physics, Indian Institute of Technology, Kanpur – 208016, India

(Received October 6, 1992)

The polycrystalline samples of copper and vanadium doped as well as undoped $(ZrO_2)_{0.8}(Y_2O_3)_{0.2}$ were synthesized and studied using X-ray diffraction, scanning electron microscopy and electron paramagnetic resonance (EPR) techniques in order to investigate their structural and magnetic behaviour. The effect of exposure to lithium vapours on the host lattice of these ceramic materials is also studied using EPR technique. It has been observed from X-ray diffraction study that the samples consist of mainly two phases monoclinic and tetragonal. The monoclinic phase is in dominant proportion. Scanning electron microscope study showed that the morphology of the samples is similar to each other. EPR studies showed interesting changes on diffusion of lithium into the lattice of the host materials.

PACS numbers: 61.16.–d, 61.10.Lx, 76.30.Fc

1. Introduction

Stabilized zirconia ZrO_2 has been the subject of great interest because of its practical applications as solid electrolytes, high technology ceramic materials and wear parts of gas turbine [1]. It has been reported that ZrO_2 has three well-defined polymorphs, namely, monoclinic, tetragonal and cubic [2]. The pure ZrO_2 may be stabilized in cubic form by the addition of variable amounts of R_2O_3 (R = rare earth or yttrium) or CaO. The phase diagram of the ZrO_2–Y_2O_3 system has indicated that the cubic phase exists in the range of composition from 6 to 40 mole% of Y_2O_3 [3]. However, in the case of ZrO_2–Y_2O_3 solid solution the stabilization of cubic phase takes place when the concentration of Y_2O_3 does not exceed 10 mole%. It has been reported that the zirconia compacts sintered at 1200°C are found to exhibit the maximal densification [4]. Manganese (II) doped $(ZrO_2)_{0.8}(Y_2O_3)_{0.2}$ single crystal has been investigated by electron paramagnetic resonance [5]. In the present investigation, the results on polycrystalline ceramic oxide samples of $(ZrO_2)_{0.8}(Y_2O_3)_{0.2}$ undoped as well as in doped forms are reported. In order to

study and correlate the structural and magnetic properties, the samples were characterized using X-ray diffraction (XRD), scanning electron microscopy (SEM) and EPR techniques. Since EPR is a sensitive technique to prove valence states and the microscopic changes around the paramagnetic ions in solids, therefore the effect of exposure to lithium vapours on the samples was studied with the help of this technique particularly.

2. Experimental

The synthesis of the stoichiometric samples in undoped as well as doped forms was performed using standard high-temperature solid state reaction route. Stoichiometric mixture of the high purity (99.99%) oxides of Zr and Y (Aldrich, USA) was thoroughly mixed and compacted into pellet form under the application of a hydrostatic pressure of ≈ 6 tonnes/cm^2. To prepare doped samples, the dopants were mixed with starting mixture. The dopants were taken in the form of nitrate for copper and in the form of oxide (V_2O_5) for vanadium. The concentration of dopant impurities was kept 1% by weight of the starting material. The pelletized materials were kept for sintering at a temperature of ≈ 1500°C in a furnace for 24 h. The samples were then furnace cooled to room temperature (RT). Thus the synthesized samples were characterized through XRD, SEM and EPR studies. The samples were also exposed to lithium vapours for various durations and temperatures to observe the effects of exposures by EPR spectroscopy. For lithium exposure samples were sealed in specially designed quartz tubes. The sample tubes were annealed at various temperatures (100 to 500°C) for different durations (15 min to 72 h). The XRD patterns were recorded on powder form using a Rich Seifert Isodebyeflex 2002 diffractometer with Cu K_α radiation. The SEM micrographs were taken using a JEOL 840 scanning electron microscope. The micrographs were taken at a magnification of $\times$ 2500. EPR measurements were performed with the help of an X-band EPR spectrometer (Varian E-109) using 100 kHz phase sensitive detection. The samples were sealed in 4 mm outer diameter quartz tubes which were kept inside a TE_{104} rectangular cavity (unloaded $Q \approx 6000$). Sample tubes were immersed in liquid nitrogen in a cold finger quartz dewar for EPR study at liquid nitrogen temperature (LNT).

3. Results and discussion

The undoped samples were designated as SZYP, the copper doped samples as SZYCu and the vanadium doped samples as SZYV. Figure 1 shows the XRD patterns of SZYP, SZYV and SZYCu samples. The patterns consist of peaks corresponding to the three known phases, namely, monoclinic, tetragonal and cubic [2]. The composition of these phases can be estimated using the following semi-empirical expressions [6, 7]:

$$W_M = \left[\frac{I_M(11\bar{1}) + I_M(111)}{I_M(11\bar{1}) + I_M(111) + I_{T,C}(111)}\right] \cdot 100, \tag{1}$$

$$W_C = (1 - W_M)\left[\frac{I_T(400) + I_T(004)}{I_T(400) + I_T(004) + I_C(400)}\right] \cdot 100 \tag{2}$$

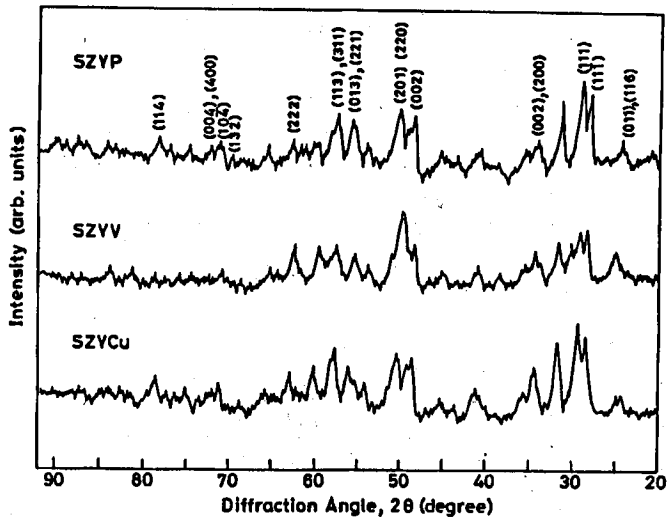

Fig. 1. X-ray diffraction patterns for samples SZYP, SZYV and SZYCu. (*hkl*) assignments for SZYP are shown.

and

$$W_C = [100 - (W_M + W_T)], \tag{3}$$

where W_M, W_T and W_C are the percentage concentrations of monoclinic, tetragonal and cubic phases, respectively and I_M, I_T and I_C are intensities of peaks of the concerned phases with the numbers in parentheses indicating the (*hkl*) assignment to the peak concerned. It is assumed here that the intensities of different peaks of respective phases represent the amount of the particular phases. The composition of these phases estimated from the above relations are collected in Table I. It may be noted from this table that in these samples monoclinic phase is the dominant one and the cubic phase exists in traces, which is consistent with the earlier observation [2]. A list of typical crystallographic parameters for the sample SZYP is given in Table II.

TABLE I

Relative phase composition along with sample code.

Sample number	Sample code	Phase composition [%]		
		Monoclinic	Tetragonal	Cubic
1	SZYP	61	33	6
2	SZYV	65	30	5
3	SZYCu	62	32	6

Figure 2 shows the SEM micrographs for the samples SZYP, SZYV and SZYCu. It is evident from the micrographs that the samples comprise two major

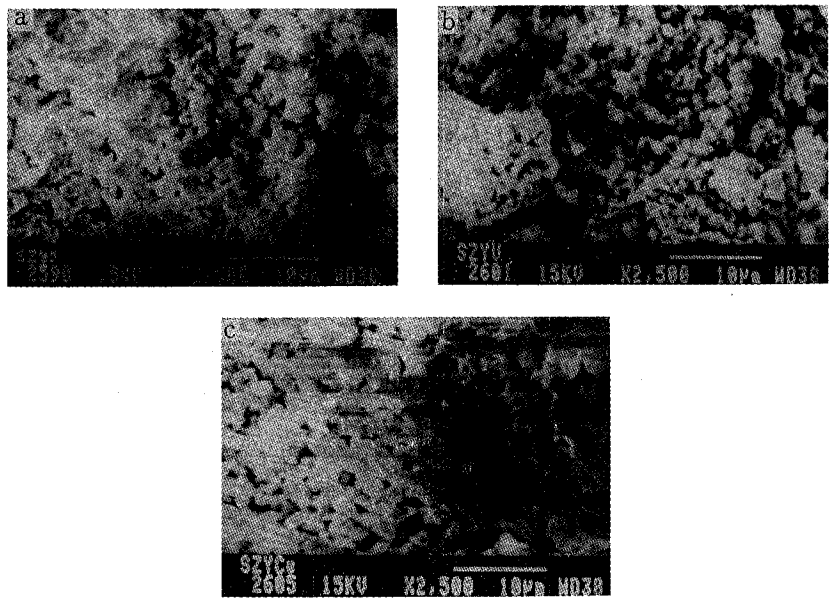

Fig. 2. Scanning electron micrographs for samples SZYP, SZYV and SZYCu. The magnification and scale are shown on the micrograph.

TABLE II

Crystallographic data estimated from XRD studies for the sample SZYP (M = monoclinic, T = tetragonal and C = cubic).

Phases	d_{obs} [Å]	d_{cal} [Å]	$d_{obs} \sim d_{cal}$ [Å]	$(I/I_0)_{obs}$ [%]	Phases	d_{obs} [Å]	d_{cal} [Å]	$d_{obs} \sim d_{cal}$ [Å]	$(I/I_0)_{obs}$ [%]
M	3.60	3.64	0.04	24	M	1.68	1.69	0.01	16
M	3.12	3.16	0.04	77	T,C,M	1.64	1.64	0.00	38
–	3.02	2.97	0.05	100	C,M	1.47	1.47	0.00	16
M	2.80	2.84	0.04	76	T	1.34	1.37	0.03	6
M,C	2.59	2.56	0.03	30	M	1.31	1.32	0.01	26
M	2.30	2.28	0.02	8	C,T	1.29	1.28	0.01	16
M	2.17	2.18	0.01	21	C	1.26	1.26	0.00	16
T	2.06	2.10	0.04	10	–	1.22	1.23	0.01	10
M	1.98	2.01	0.03	20	T	1.21	1.21	0.00	20
M	1.86	1.85	0.01	70	T	1.10	1.10	0.00	11
T,M	1.80	1.81	0.01	72	T	1.09	1.09	0.00	9

phases in conformity with XRD observation. These micrographs show inhomogeneous microstructure of the phases. The average grain size seems to vary from sample to sample. Generally, sintering temperature, duration and synthesis routes are the factors which affect the microstructure of the final product. It should be

stressed here that we followed identical heat treatments for the samples under study. Therefore, the variation in average size may be attributed to the effect of dopants.

The EPR spectra of the finally crushed samples SZYP, SZYV and SZYCu are shown in Fig. 3. The EPR spectrum of the sample SZYP comprises a narrow resonance line (marked as P) near $g \approx 2$ superimposed on a broader signal (marked as b). The narrow signal is situated at $g_P = 1.975 \pm 0.005$ and the peak-to-peak

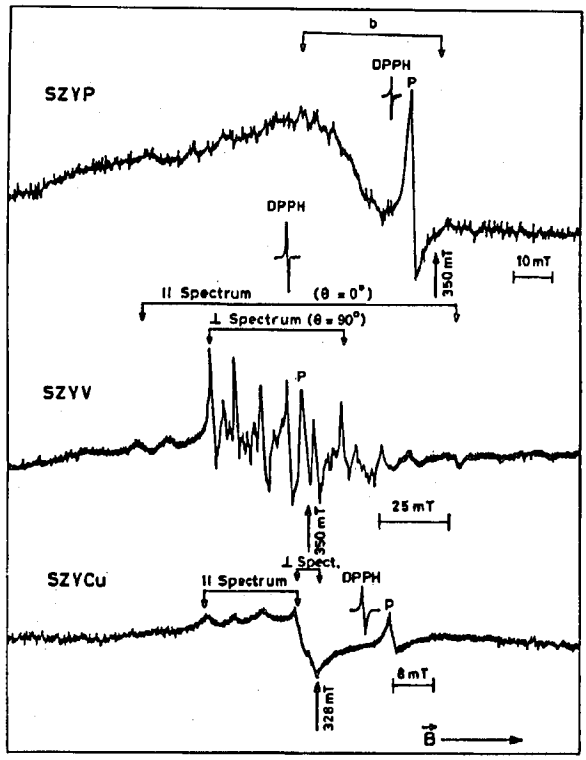

Fig. 3. EPR spectra of samples SZYP, SZYV and SZYCu at X band and at RT.

(p–p) width of this signal $\Delta H_P \approx 25 \pm 3$ G. The p–p width of the broader signal $\Delta H_b \approx 290 \pm 30$ G and it is situated around $g_b \approx 2.05$. Since we took 99.99% pure constituents for synthesizing the SZYP sample, therefore, the presence of any extrinsic paramagnetic impurity is not expected. However, the sample indicates the presence of some paramagnetic centres. Though it was not possible to identify the exact nature and cause of these centres, the presence of these paramagnetic species may be an artefact of synthesis process in the present case. Another interesting aspect of these signals is that their widths and positions remain essentially temperature independent between RT and LNT. It is also interesting to recall that XRD and SEM studies revealed the presence of two major phases in this sample. The two EPR signals observed may originate from these phases.

The sample SZYV has displayed eight-line EPR spectrum (Fig. 3) which is discussed below. It is well known that vanadium has three oxidation states (V^{2+}, V^{3+} and V^{4+}). V^{4+} is isoelectronic with Ti^{3+} and favours an octahedral coordination with oxygen. However, one V–O bond is usually much shorter than the rest in the VO_6 octahedron. Thus V^{4+} is subjected to a crystal field of compressed tetragonal character. Tetravalent vanadium is found to form VO^{2+} (vanadyl) ion, i.e. V^{4+} in close association with O^{2-} favourably [8]. Vanadyl ion and its complexes contain one unpaired electron to give EPR spectrum. The g factor lies between 1.9 and 2. In magnetically dilute system V^{4+} and VO^{2+} show a fairly large hyperfine splitting due to ^{51}V which has nuclear spin $I = 7/2$ (99.8% abundant). The EPR results may be interpreted in terms of the following spin Hamiltonian with $S = 1/2$ and $I = 7/2$:

$$\mathcal{H} = \beta \boldsymbol{S} \cdot \tilde{\tilde{g}} \cdot \boldsymbol{B} + \boldsymbol{I} \cdot \tilde{\tilde{A}} \cdot \boldsymbol{S}. \tag{4}$$

Trivalent vanadium has an electronic structure $3d^2$. The ^3F free ion ground state is split by an octahedral coordination leaving an orbital triplet (T_2) lowest. The trigonal component of the crystal field further splits this to give an orbital singlet ground state. The threefold spin degeneracy is lifted by the combined effect of trigonal field and spin–orbit coupling. EPR signal may be observed from $m_s = \pm 1$ states with $g_{\|} \approx 1.9$ and the resonance field may be expressed approximately by

$$B_0 = \frac{h\nu}{2g_{\|}\beta\cos\theta}, \tag{5}$$

where θ is the angle between magnetic field and the trigonal axis [9]. The divalent vanadium with d^3 electronic configuration would give an EPR spectrum comprising three sets of eight lines each (octets) in an distorted octahedral environment. On the basis of the above discussion we may attribute the observed EPR spectrum of vanadium doped sample SZYV to the tetravalent vanadium (possibly vanadyl form of V^{4+} ion). The observed spectrum resembles typical powder spectra of vanadyl complexes having axial symmetry [10]. For the axial symmetry the resonance fields are given by [11–13]:

$$B_m = B_0 - \frac{Km}{g\beta} - [I(I+1) - m^2]\frac{A_{\perp}^2(A_{\|}^2 + K^2)}{4B_0K^2(g\beta)^2} - \left(\frac{A_{\|}^2 - A_{\perp}^2}{K}\right)^2 \left(\frac{g_{\|}g_{\perp}}{g^2}\right)^2 \frac{m^2\sin^2 2\theta}{8g^2\beta^2B_0}, \tag{6}$$

where

$$B_0 = \frac{h\nu}{g\beta}, \quad g^2 = g_{\|}^2\cos^2\theta + g_{\perp}^2\sin^2\theta, \quad K^2g^2 = A_{\|}^2g_{\|}^2\cos^2\theta + A_{\perp}^2g_{\perp}^2\sin^2\theta,$$

B_m denotes the resonance field for the transition $m \longleftrightarrow m$ and m varies from $7/2$ to $-7/2$, and θ is the angle between V–O bond of the vanadyl ion and the applied magnetic field $\boldsymbol{B}$. After identifying the lines corresponding to $\theta = 0°$ ($\|$-spectrum) and $\theta = 90°$ ($\perp$-spectrum) in the powder EPR spectrum shown in Fig. 3 spin-Hamiltonian parameters viz. $g_{\|}$, $g_{\perp}$, $A_{\|}$ and $A_{\perp}$ were calculated in

units of $(g\beta)^{-1}$ [gauss] using above expressions and are given in Table III. These parameters are in good agreement with the values for vanadyl complexes [13]. Therefore, the vanadium impurity seems to enter the host lattice in the form of a vanadyl complex. The possible site may be Zr^{4+} having an octahedral environment of oxygens. The powder EPR spectrum of the copper doped samples SZYCu is also

TABLE III

Parameters derived from EPR studies.

Sample code	g values	Hyperfine parameters A [gauss]	Line width ΔH [gauss]
SZYP	$g_P = 1.975 \pm 0.005$	–	$\Delta H_P = 25 \pm 3$
	$g_b = 2.05 \pm 0.05$	–	$\Delta H_b = 290 \pm 30$
SZYV	$g_P = 1.975 \pm 0.005$	$A_\parallel = 166 \pm 5$	$\Delta H_P = 25 \pm 3$
	$g_\parallel = 1.935 \pm 0.005$		
	$g_\perp = 1.980 \pm 0.005$	$A_\perp = 66 \pm 5$	–
SZYCu	$g_P = 1.975 \pm 0.005$	$A_\parallel = 56 \pm 5$	$\Delta H_P = 22 \pm 3$
	$g_\parallel = 2.175 \pm 0.005$		
	$g_\perp = 2.037 \pm 0.005$	$A_\perp = 24 \pm 5$	–

shown in Fig. 3. Cu^{2+} with $3d^9$ configuration may be regarded as a single hole in the filled $3d^{10}$ configuration. Its EPR would be similar to d^1 configuration. Since the two naturally occurring isotopes of copper (^{63}Cu and ^{65}Cu) have nuclear spins $I = 3/2$, the EPR spectra are explained by the spin Hamiltonian of Eq. (4) with $S = 1/2$ and $I = 3/2$ [14]. In an axial crystalline field the positions of resonance lines are expressed by Eq. (6) with the difference that here m varies from $3/2$ to $-3/2$. The values of $g_\perp$, $g_\parallel$, $A_\perp$ and $A_\parallel$ are listed in Table III. Since $g_\parallel > g_\perp > 2$, hence the unpaired electron resides in $d_{x^2-y^2}$ ground state orbital of the Cu^{2+} ion and the ion experiences an axial crystalline field in the host lattice. The site of Cu^{2+} ions may be an interstitial one or a substitutional one and would require some charge compensation mechanism in both the cases in the present host.

All the samples were exposed to lithium vapours to investigate the effects of lithium diffusion in the host matrix through changes in the EPR spectra. No discernible changes in EPR spectra are seen when exposure temperature is kept below 400°C. However, at temperature above 400°C discernible changes are noticed for some samples. The sample SZYP does not depict discernible changes in the whole range of exposure (up to 500°C and 72 h). The noticeable difference for SZYV was that while intensity of resonance signals decreased significantly on exposure (500°C/72 h), the other feature remained essentially the same. The sample SZYCu exposed to lithium at 500°C for 72 hours displayed remarkable changes in EPR spectra as shown in Fig. 4. The EPR signal becomes extremely broad and asymmetric after exposure making the measurements of g and ΔH impossible.

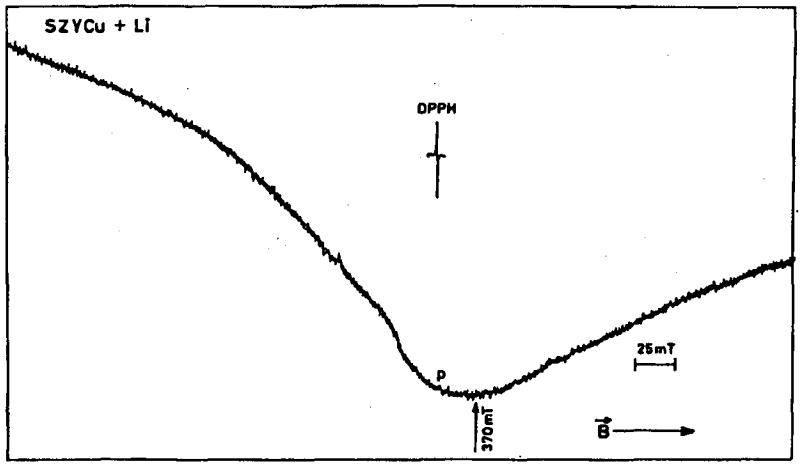

Fig. 4. X-band EPR spectrum at RT of sample SZYCu exposed to lithium vapours at 500°C for 72 h.

The broadening of signal indicates changes in the local environment of the Cu^{2+} ions. A faster relaxation time may be the cause for the broadening of the EPR signal. Alternatively, the precipitation of copper impurity may be the cause for a broad EPR signal due to dipolar broadening in concentrated paramagnetic phase.

4. Conclusion

The results of EPR, SEM and XRD investigations of $(ZrO_2)_{0.8}(Y_2O_3)_{0.2}$ samples prepared by solid state reaction method show that the favourable phases are monoclinic and tetragonal. Small amounts of vanadium and copper impurities are not found to change the composition of the system noticeably. However, EPR studies reveal that vanadium and copper enter the host lattice in paramagnetic valence states. The vanadium impurity seems to form a vanadyl complex and is believed to replace Zr^{4+} ions at octahedral sites. The copper ion is in Cu^{2+} state and its ground state is $d_{x^2-y^2}$. The Cu^{2+} ion is subjected to an axially distorted octahedral crystalline field at the site of incorporation in the host lattice. Lithium seems to diffuse in the host lattice at higher temperatures and it seems to affect the copper impurity complex significantly. A possible segregation of copper impurity caused by lithium diffusion is proposed.

Acknowledgment

One of the authors (N.L.S.) is thankful to the University Grants Commission, India for providing financial support in the form of teacher fellowship.

References

[1] R. Stevens, in: *Handbook of Ceramics*, Supplement to *Inter. Ceram.* **34**, 1 (1985).

[2] N. Iwamoto, N. Umeski, S. Endo, *Thin Solid Films* **127**, 129 (1985).

[3] E.A. Zhilinskaya, V.N. Lazukin, I.V. Chepeleva, in: *Magnetic Resonance and Related Phenomena*, Eds. E. Kundla, E. Lippmaa, T. Saluvere, Springer, Berlin 1979, p. 325.

[4] N.M. Ghoneim, S.B. Hanna, *J. Mater. Sci.* **25**, 5192 (1990).

[5] M. Stempi, H. Szymczak, A.A. Andreev, *Acta Phys. Pol. A* **63**, 627 (1983).

[6] S.V. Sharma, P. Chand, *Acta Phys. Pol. A* **81**, 653 (1992).

[7] B.D. Cullity, *Elements of X-ray Diffraction*, Addison Wesley, California 1978.

[8] C.J. Ballhausen, *Introduction to Ligand Field Theory*, McGraw-Hill, New York 1962.

[9] J.W. Orton, *Electron Paramagnetic Resonance*, Iliffe Books Ltd., London 1968.

[10] J.E. Wertz, J.R. Bolton, *Electron Spin Resonance*, McGraw-Hill, New York 1972.

[11] B. Bleaney, *Philos. Mag.* **42**, 441 (1951).

[12] A. Abragam, B. Bleaney, *Electron Paramagnetic Resonance of Transition Ions*, Clarendon Press, Oxford 1970.

[13] P. Chand, V.K. Jain, G.C. Upreti, *Magn. Reson. Rev.* **14**, 49 (1988).

[14] A. Carrington, A.D. McLachlan, *Introduction to Magnetic Resonance*, Chapman & Hall Ltd., London 1979.